Journal of Nuclear Medicine, published on February 24, 2022 as doi:10.2967/jnumed.121.263453

Administration Routes for SSTR- / PSMA- and FAP-directed Theranostic Radioligands in Mice

Running title: Biodistribution of ^{68}Ga-ligands

Jasmin M. Klose[1], Jasmin Wosniack[1], Janette Iking[1], Magdalena Staniszewska[1], Fadi Zarrad[1], Marija Trajkovic-Arsic[2,3], Ken Herrmann[1], Pedro Fragoso Costa[1], Katharina Lueckerath[1,4], Wolfgang P. Fendler[1]

[1] Department of Nuclear Medicine, University Hospital Essen, University of Duisburg-Essen, Essen, Germany

[2] Division of Solid Tumor Translational Oncology, German Cancer Consortium (DKTK), partner site Essen, West German Cancer Center, University Hospital Essen, Essen, Germany

[3] German Cancer Consortium (DKTK) and German Cancer Research Center (DKFZ), Heidelberg, Germany.

[4] Ahmanson Translational Theranostics Division, Department of Molecular & Medical Pharmacology, David Geffen School of Medicine, University of California Los Angeles, USA.

Corresponding author:
Wolfgang Peter Fendler, M.D.
Address: Hufelandstraße 55, 45147 Essen, Germany
Telephone number: +49 201 723 2032
E-mail: Wolfgang.Fendler@uk-essen.de

First author:
Jasmin Mona Klose, PhD
Address: Hufelandstraße 55, 45147 Essen, Germany
Telephone number: +49 201 723 2032
E-mail: Jasmin.Klose@uk-essen.de

Word count: 4779

ABSTRACT

Introduction: The NETTER-1, VISION, and TheraP trials prove efficacy of repeat intravenous (i.v.) application of small radioligands. Application by subcutaneous (s.c.), intraperitoneal (i.p.), or oral (p.o.) access are important alternatives and may yield comparable or favorable organ and tumor radioligand uptake. Here, we assess organ and tumor biodistribution for various radioligand application routes in healthy mice and models of somatostatin receptor (SSTR)-, prostate-specific membrane antigen (PSMA)-, and fibroblast activation protein (FAP)- expressing cancer.

Methods: Healthy and tumor-bearing male C57BL/6 or NOD SCID Gamma mice, respectively, were applied with a mean of 6.0±0.5 MBq ^{68}Ga-DOTATOC (RM1-SSTR allograft), 5.3±0.3 MBq ^{68}Ga-PSMA11 (RM1-PSMA allograft) or 4.8±0.2 MBq ^{68}Ga-FAPI46 (HT1080-FAP xenograft) i.v., i.p., s.c. or p.o.. *In vivo* positron emission tomography and *ex vivo* biodistribution in tumor, organs, and at the injection site were assessed up to 5h post injection (p.i.). Healthy mice were monitored for up to 7 days after the last scan for signs of stress or adverse reactions.

Results: After i.v., i.p. and s.c. radioligand administration, average residual activity at the injection site was <17%IA/g (1h p.i.), <10%IA/g (2h p.i.) and ≤4%IA/g (4h p.i.) for all radioligands. Following oral administration ≥50%IA/g remained within the intestines until 4h p.i.. Biodistribution in organs of healthy mice was nearly equivalent following i.v., i.p., and s.c. application at 1h p.i. and all subsequent timepoints (≤1%IA/g for liver, blood and bone marrow; 11.2±1.4%IA/g for kidneys). In models for SSTR-, PSMA- and FAP-expressing cancer, tumor uptake was higher or equivalent for i.p./s.c. versus i.v. injection at 5h p.i. (*ex vivo*): SSTR: 7.2±1.0%IA/g (p=0.0197) / 6.5±1.3%IA/g (p=0.0827) versus 2.9±0.3%IA/g; PSMA: 3.4±0.8%IA/g (p=0.9954) / 3.9±0.8%IA/g (p=0.8343) versus 3.3±0.7%IA/g and FAP: 1.1±0.1%IA/g (p=0.9805) / 1.1±0.1%IA/g (p=0.7446) versus 1.0±0.2%IA/g.

Conclusion: In healthy mice, biodistribution of small theranostic ligands following i.p. or s.c. application is nearly equivalent compared to i.v. injection. S.c. administration resulted in highest absolute SSTR tumor and tumor-to-organ uptake as compared to the i.v. route, warranting further clinical assessment.

Keywords:

radioligand, biodistribution, small animal PET, theranostic, intravenous, subcutaneous, intraperitoneal, PSMA, SSTR, FAP, alternative application routes

INTRODUCTION

NETTER-1 (*1*), and the more recent clinical trials TheraP (*2*), and VISION (*3*), establish somatostatin receptor (SSTR)- and prostate specific membrane antigen (PSMA)-directed small ligand radiotheranostics as efficacious cancer therapy with favorable safety profiles. Recently, fibroblast activation protein (FAP)-targeting small ligands have emerged for positron emission tomography (PET) and therapy of cancers (*4*). Intravenous (i.v.) application is the standard route for radioligand applications. However, oral (p.o.), intraperitoneal (i.p.), and subcutaneous (s.c.) administrations are faster and require a lower level of training when compared to i.v., both in the preclinical and clinical settings. The volume of preclinical and clinical radioligand applications is growing rapidly and thus, there is an urgent unmet need to assess alternative application routes to address the increasing demand. In addition, novel FAP-directed therapies are in a dynamic and evolving process, highlighting the emerging need for an optimization of administration routes of these novel radioligands for ongoing preclinical and clinical assessment. In this intent, assessment of biodistribution and administration routes of ^{68}Ga-FAPI46 (fibroblast activation protein inhibitor) was requested by the German Federal Institute for Drugs and Medical Devices (BfArM) for recent approval of a prospective clinical trial on ^{68}Ga-FAPI46 PET/CT for various types of cancer (NCT04571086).

We hypothesize that i.p. and s.c. application will yield near equivalent organ and tumor biodistribution compared to the routine i.v. injection. We further hypothesized that organ and tumor uptake will be significantly lower following p.o. application of radioligands. Here, we compare tumor and organ biodistribution following i.v., i.p., s.c and p.o. application of small radioligands in healthy mice and mouse models of SSTR-, PSMA-, and FAP-expressing cancer.

METHODS

Cell Culture

RM1 cells, virally stably transduced with SFG-Egfp/Luc (RM1-PGLS) or pMSCV-IRES-YFP II-hSSTR (RM1-SSTR) to express high levels of cell surface human PSMA or SSTR2 (*5*), were obtained from Johannes Czernin (University of California, Los Angeles). HT1080-FAP cells were a gift from Uwe Haberkorn (University Hospital of Heidelberg). HT1080 cells were stably transfected with the plasmid pcDNAI/neo-FAP (expressing the untagged full-length cDNA of human FAP) followed by neomycin selection (*6*). RM1-PSMA and RM1-SSTR were maintained in Roswell Park Memorial Institute 1640 medium (GIBCO) and HT1080-FAP in Dulbecco's Modified Eagle Medium (GIBCO), both with 10% fetal bovine serum (Thermo Fisher Scientific) and 0.5% penicillin/streptomycin (GIBCO), at 37°C with 5% CO_2. Cells were thawed 2 weeks or passaged 3 times before inoculation. Cells were routinely assessed for mycoplasma contamination using the VenorGeM OneStep kit (Minerva Biolabs).

Radiosynthesis

^{68}Ga-DOTATOC, ^{68}Ga-PSMA11 and ^{68}Ga-FAPI46 were obtained from the radiopharmacy of our clinic. Clinical-grade radiolabeling of precursors (DOTATOC, PSMA11, FAPI46) was performed using the Modular-Lab eazy for DOTATOC and PSMA or Scintomics GRP 3V for FAPI using commercially available reagent kits. The final solution had <5µg/mL for ^{68}Ga-DOTATOC, <3µg/mL for ^{68}Ga-PSMA, and ~50µg/mL for ^{68}Ga-FAPI with 100µl injected volume per mouse. Radiochemical purity was determined with radio-high-performance liquid chromatography. FAPI: Chromolith Performance RP18e column from Merck (100 x 3mm) gradient: 0-20% MeCN+0.1% TFA in 5 min run time 15 min; PSMA: 5-40% MeCN+0.1% TFA in 10 min run time 15 min; DOTATOC: 24% MeCN+0.1% TFA for 8 min, then 24-60% in 1 min, run time 15 min; and thin-layer chromatography (iTLC-SG, ammonium acetate (77g/L), methanol R (50:50 v/v)). The radiochemical purity exceeded 98% for all radioligands.

Mice and Tumor Models

Male C57BL/6 and NOD SCID Gamma mice were purchased from Charles River Laboratories (6-8 weeks old) and housed under specific pathogen-free conditions with food and

water available *ad libitum*. Health status monitoring of mice was performed by assessing a summarized score twice a week (healthy animals) or daily (tumor-bearing animals). The study was approved by the North Rhine-Westphalia State Agency for Nature, Environment and Consumer Protection (LANUV), Germany (permit number: AZ.81-02.04.2018.A090).

For subcutaneous tumors, mice were injected with 0.1×10^6 RM1-SSTR cells or RM1-PSMA (C57BL/6) or 1.0×10^6 HT1080-FAP (NOD SCID Gamma) in matrigel/PBS (50:50 ratio) into the shoulder region. Tumor volume (*V*) was calculated by measuring the length (*L*) and width (*W*) of tumors by caliper and using the formula $V = 1/2(L \times W^2)$ (*7*). PET scans were acquired 7-10 days after tumor inoculation, as described previously (*5,8*). Mean+SEM tumor volumes were 0.39±0.09cm³ (interquartile range 0.07-0.66cm³) for RM1-SSTR tumors, 0.05±0.01cm³ (interquartile range 0.02-0.08cm³) for RM1-PSMA tumors, and 0.22±0.03cm³ (interquartile range 0.06-0.25cm³) for HT1080-FAP tumors.

Radioligand Application and Small Animal Positron Emission Tomography/Computed Tomography (PET/CT)

Healthy or tumor-bearing anesthetized mice (1.5-2% isoflurane) received (mean±SEM) 6.0±0.5 MBq ^{68}Ga-DOTATOC, 5.3±0.3 MBq ^{68}Ga-PSMA11 or 4.8±0.2 MBq ^{68}Ga-FAPI46 i.v. (tail vein), i.p., s.c. or p.o. (p.o. HT1080-FAP tumor-bearing mice only) (differences between injected activities, p=n.s.). Each healthy mouse received i.v., i.p., s.c. and p.o. administration with 1 week interval between PET/CT scans (Supplemental Figure 1A). Each tumor-bearing mouse was scanned twice, at 1h and 4h p.i., following either i.v., i.p., or s.c. application and was sacrificed ~5h p.i for *ex vivo* analysis (Supplemental Figure 1B). Imaging was performed with a β-CUBE (PET) and X-CUBE (CT) (Molecubes) in temperature-controlled beds with monitoring of breathing frequency. PET/CT was acquired (PET, 15 minutes; CT, 5 minutes) in list mode with frames for 5, 10 and 15 minutes (dynamic scans, maximum delay between injection and scan start 5 minutes) and static scans 1h, 2h and 4h p.i. for healthy mice and 1h and 4h p.i. for tumor groups.

Image Reconstruction and Processing

Images were reconstructed using an iterative reconstruction algorithm (ISRA, 30 iterations) with attenuation correction of the corresponding CT image. PET data were reconstructed into a 192x192 transverse matrix, producing a 400 µm isometric voxel size. PET images were evaluated with PMOD software (PMOD Technologies LLC). Decay-corrected mean percent injected activity

per gram (%IA/g) of the tumor and organs of interest was derived from DICOM images. Volumes of interest (VOIs) were defined as spheres of 5 mm (lung, liver, spleen, intestines, heart, brain, kidneys) and 2.5 mm (bone marrow, thigh muscle, blood pool, injection site, tumor) diameter in tissues of interest. %IA/g was calculated from the average pixel values reported in Bq/mL within these VOIs corrected for radioactive decay and mouse body weight.

Ex Vivo Analysis

Approximately 5h p.i., animals were sacrificed and organs of interest were extracted, dabbed dry, weighed, and radioactivity was measured in an automated gamma counter (Perkin-Elmer Gamma Counter 2480 Wizard²). Organ and tumor uptake was calculated from radioactive counts, decay-corrected and expressed as %IA/g.

Data and Statistical Analysis

Data are presented as mean±SEM unless indicated otherwise. All statistical analyses were performed using GraphPad Prism (version 9.1.0; GraphPad Software). Tumor-to-organ uptake ratios were calculated for blood, kidney, liver and bone marrow (femur) using %IA/g at 1h and 4h in *in vivo* VOIs and at 5h for *ex vivo* gamma counter measurements (%IA/g tumor / %IA/g organ). Statistical significance was assessed using Brown-Forsythe and Welch ANOVA test with Dunnett's T3 multiple comparisons test or Tukey's multiple comparisons test. p-values below 0.05 were considered statistically significant. Statistically significant data are indicated by asterisks (*p<0.05; **p<0.01; ***p<0.001; ****p<0.0001).

RESULTS

Local and Systemic Activity

To assess biodistribution of radioligands applied via different routes, we measured the activity retained at the injection site versus the overall systemic activity distribution excluding the application site. Activity at the injection site decreased over time following i.v., i.p. and s.c. administration in healthy mice (Figure 1, Supplemental Figure 1). Residual activity at the injection site 4h p.i. was (mean±SEM) for i.v.: 1.0±0.3%IA/g, i.p.: 4.4±2.1%IA/g and s.c.: 2.1±0.5%IA/g) for all radioligands; this correlated inversely with increased systemic availability of radioligands. Oral administration resulted in significant and prolonged retention of radioligands in the stomach and proximal small bowel as well as a low systemic distribution (Figure 1A-C). Following p.o. administration, average systemic uptake was highest for ^{68}Ga-FAPI46 (Figure 1C). Therefore, p.o. application was further explored in HT1080-FAP tumor-bearing mice.

Near Equivalent Organ Biodistribution of Radioligands Following i.p., s.c., and i.v. Application in Healthy Mice

In healthy mice, i.p., s.c., and i.v. injection of radioligands resulted in near equivalent organ biodistribution *in vivo* (Figure 2-4, Supplemental Figures 2-3). Radioligand retention in blood and kidney is listed in Supplemental Table 1. Blood retention in healthy mice was significantly higher following i.p. or s.c. versus i.v. application of ^{68}Ga-PSMA11: i.p., 1h p=0.0226, 2h p=0.0463, and 4h p=0.0394; s.c., 1h p=0.0880, 2h p=0.0021, and 4h p=0.065. For ^{68}Ga-DOTATOC and ^{68}Ga-FAPI46, blood and kidney distribution after i.p. and s.c. application were comparable to those following i.v. injection (Figure 2-4). In further organs, including liver, bone marrow, lung, heart spleen, intestines, brain and muscle, i.p., s.c., and i.v. application routes exhibited comparable physiological biodistribution (Supplemental Figure 2). Moreover, in healthy mice, no short-term and longer-term adverse effects of radioligand application and PET/CT procedures were noted during the study duration (5 weeks).

Increased or Comparable Tumor Uptake Following i.p. or s.c. Versus i.v. Injection of Radioligands

To evaluate the impact of the application route on tumor uptake of ^{68}Ga-DOTATOC, ^{68}Ga-PSMA11, or ^{68}Ga-FAPI46, we assessed *in vivo* and *ex vivo* tumor and organ uptake in SSTR-, PSMA- and FAP-expressing tumor models (Table 1, Figure 5-7, Supplemental Figures 4-5).

In mice bearing SSTR tumors, i.p./s.c. application resulted in significantly higher tumor uptake (mean±SEM) when compared to i.v.: p=0.0124 / p=0.0377 at 1h; p=0.0301 / p=0.0411 at 4h; and p=0.0197 / p=0.0827 at 5h (*ex vivo*) (Table 1; Supplemental Figure 4). Tumor uptake of ^{68}Ga-PSMA11 or ^{68}Ga-FAPI46 following i.p./s.c. injection of mice bearing PSMA- or FAP-expressing tumors was comparable to the uptake observed after i.v. injection (Table 1).

Oral administration in mice bearing FAP-expressing tumors did not result in notable tumor uptake (Table 1, Supplemental Figure 4). Oral application of ^{68}Ga-FAPI46 in tumor-bearing mice yielded comparable biodistribution characteristics as seen in healthy mice (Supplemental Figure 4) with high gastrointestinal retention of the radioligand and low systemic distribution.

Tumor-to-organ uptake ratios of organs relevant for dosimetry (*9,10*) for i.p./s.c. versus i.v. application are depicted in Figure 5-7. I.p./s.c. application resulted in higher or equivalent tumor-to-liver ratios at 5h p.i. when compared to i.v. (5h p.i. mean ratio±SEM): (i) ^{68}Ga-DOTATOC: 27.4±2.2-fold (p=0.0138) / 25.3±5.6-fold (p=0.2756) versus 13.9±2.9-fold; (ii) ^{68}Ga-PSMA11: 28.2±7.4-fold (p=0.4504) / 39.4±5.7-fold (p=0.0259) versus 16.9±2.8-fold; and (iii) ^{68}Ga-FAPI46: 6.1±1.6-fold (p=0.4198) / 12.0±1.1-fold (p=0.0005) versus 3.7±0.4-fold (Figure 5-7). Tumor-to-bone marrow ratios were higher for i.p. compared with i.v. application in mice bearing SSTR-expressing tumors: 50.7±4.3 versus 25.7±4.9 (p=0.0096) (Figure 5). S.c. application resulted in higher tumor-to-blood ratios when compared with i.v. application in mice bearing PSMA-expressing tumors: 24.5±4.2-fold versus 6.0±0.9-fold (p=0.0186). For other tumor-to-organ uptake ratios no significant difference was observed (Figure 6). Oral application of ^{68}Ga-FAPI46 resulted in negligible uptake in organs and tumors (Table 1, Supplemental Figure 4).

DISCUSSION

The current delivery method for radioligands for nuclear imaging or therapy is i.v. injection. However, comparing different application routes is important for the translation of novel FAP ligands and optimization of current clinical protocols for PSMA or SSTR ligands.

The current study aimed at comparing the biodistribution of SSTR-, PSMA-, and FAP-directed small radioligands administered i.p., s.c., or p.o. with the standard i.v. application. Alternative application routes may alter systemic distribution and tumor uptake (*11-13*), for instance by slowing absorption due to a reduced rate of molecular transport via the lymphatics and blood flow to the organs of interest/tumor (*14*).

Administration of small radioligands i.v., i.p., and s.c. was feasible and well tolerated as assessed by a scoring system including behavior and overall physical appearance of mice. Small radioligand systemic availability and biodistribution was comparable for i.p. and s.c. versus i.v. application (Figure 1-4). In addition, i.p. and s.c. administration in mice resulted in significantly higher ^{68}Ga-DOTATOC tumor uptake (Table 1), tumor-to-liver and tumor-to-bone marrow ratio in SSTR-expressing tumors when compared with i.v. injection (Figure 5).

These findings have implications for preclinical and clinical radioligand administration, since they could offer advantages for both fields. In mice, i.v. injection requires highly trained personnel, and is more error-prone (e.g., paravenous injection) and time consuming. I.p. and s.c. administration may serve as simple alternative application routes for imaging at later timepoints after injection or therapy, allowing a higher throughput in mouse studies, with lower dropout rates and high reproducibility. In mice, i.p. administration did not compromise radioligand tumor accumulation despite a high initial absorbed dose in the intestines (*15*). However, due to slower systemic bioavailability following i.p. or s.c. injection, i.v. application is recommended for early dynamic imaging.

In clinical routine, usage of alternative application routes to i.v. may improve outpatient care and benefit potential new therapy schemes allowing repeat radioligand application at short interval.

In patients, i.p. application is limited due to a higher likelihood of infection or abdominal organ damage. However, s.c. application is already well established as a standard route for outpatient injectable medications and has an emerging role in delivery of biotherapeutics or monoclonal antibodies (*16,17*). Indeed, in patients with accidental paravenous infusion of ^{177}Lu-DOTATOC absorption from the paravenous injection site occurs with a half-life of less than 4h (Supplemental Figure 6); this is in line with a short drainage observed following s.c. injection in mice. We therefore expect that s.c. application in patients would be feasible.

Still, an increased radiation dose to organs such as kidneys, bone marrow, blood, lungs or liver, may limit benefit from i.p./s.c. injection. However, if radioligand therapy regimens would be changed to a weekly or biweekly schedule using s.c. application, activities for each administration could probably be reduced in favor of these more frequent treatments. Weekly or biweekly i.p./s.c. application could be realized by outpatient care, reducing the patient's time in hospital, personnel capacities and thus, reduced costs.

In this study, the uptake in non-target tissues did not exceed critical values or radiation dose as suggested from measured uptake in %IA/g (Figure 2-4). Therefore, we assume that a detrimental radiation burden to organs at risk (mainly kidneys) after s.c. and i.p. application when compared to the standard i.v. route is unlikely. Notably, preclinical and clinical studies for DOTATOC- and PSMA-targeting radiotherapies demonstrated that after i.v. absorbed doses in organs of risk are not likely to cause relevant radiotoxicity (*9,10,18,19*). However, to precisely estimate the additional absorbed dose to the adjacent tissue (by i.p. and s.c.) following radioligand therapy, further studies with Lu-177 labeled ligands and quantitative preclinical SPECT imaging should be performed. Yet, if we assume a half-life of 2.3 hours for the change in local activity over time at the injection site, as recently published by Tylski (*20*), we would not expect to detect a change in dosimetry between one Lu-177 administration and, e.g., 2-3 administrations spaced by 48 h.

To date, the entire theranostics routine is based on rather conservative application schemes with few possibilities of patient-specific modification. Our observation that s.c. application showed similar tumor uptake as compared to i.v. may open up new opportunities for alternative application schemes in the clinical routine – e.g., weekly or biweekly applications, which are less feasible if using repeat i.v. injections. Also, s.c. application is faster and easier than i.v., and could thus be realized in outpatient care by medical laboratory assistants in a time-efficient manner for both, patient and clinic personnel. Furthermore, it would be interesting to investigate the influence of i.v. application rate (applied dose per time) on tumor uptake. This could be realized in a clinical study or observational trial on patients with poor vein status.

This study has some limitations. This study assessed ^{68}Ga-ligands for PET imaging and did not examine therapeutic ^{177}Lu-labelled ligands. Furthermore, in-bed injection with concurrent dynamic PET acquisition was not performed and due to the short ^{68}Ga half-life, timepoints beyond 5h p.i. were not feasible.

CONCLUSION

In mice, PET imaging after i.v., i.p., or s.c. injection of SSTR-. PSMA-, or FAP-directed small radioligands is feasible. I.p. and s.c. administration of SSTR-ligands resulted in higher absolute tumor and relative tumor-to-organ uptake compared to i.v., which may translate into improved tumor irradiation in the setting of radioligand therapies and warrants further translational assessment.

DISCLOSURE

WPF was a consultant for Janssen and Calyx, and he received fees from Bayer and Parexel outside of the submitted work. KH reports personal fees from Bayer, personal fees and other from Sofie Biosciences, personal fees from SIRTEX, non-financial support from ABX, personal fees from Adacap, personal fees from Curium, personal fees from Endocyte, grants and personal fees from BTG, personal fees from IPSEN, personal fees from Siemens Healthineers, personal fees from GE Healthcare, personal fees from Amgen, personal fees from Novartis, personal fees from ymabs, personal fees from Aktis Oncology, personal fees from Theragnostics, personal fees from Pharma15, outside the submitted work. KL reports paid consulting activities for Sofie Biosciences/iTheranostics, and funding from AMGEN outside of the submitted work. No other potential conflict of interest relevant to this article was reported.

ACKNOWLEDGMENTS

We thank Prof. Dr. med Uwe Haberkorn for providing HT1080-hFAP cells, and the Nuclear Medicine team at University Hospital Essen for their support. This study was funded in parts by the Doktor Robert Pfleger-Stiftung, Hallstadt, Germany.

KEY POINTS

QUESTION: Are there alternatives to intravenous injection of SSTR-, PSMA-, or FAP-directed radioligands?

PERTINENT FINDINGS: In healthy mice, i.p. and s.c. application of small radiotheranostic ligands resulted in near equivalent systemic availability and organ biodistribution at early (1h) and late (4h) timepoints p.i. when compared to i.v. injection. I.p./s.c. administration significantly increased absolute tumor and relative tumor-to-organ uptake in SSTR tumors (^{68}Ga-DOTATOC) compared to i.v. route.

IMPLICATIONS FOR PATIENT CARE: I.p. and s.c. application is feasible in animal models of small radioligand imaging or therapy. Tumor uptake and tolerability of s.c. application warrants assessment in clinical studies.

REFERENCES

1. Strosberg J, Wolin E, Chasen B, et al. NETTER-1 phase III in patients with midgut neuroendocrine tumors treated with 177Lu-Dotatate: Efficacy and safety results. *J Nucl Med.* 2016;57:629-629.

2. Hofman MS, Emmett L, Sandhu S, et al. [(177)Lu]Lu-PSMA-617 versus cabazitaxel in patients with metastatic castration-resistant prostate cancer (TheraP): a randomised, open-label, phase 2 trial. *Lancet.* 2021;397:797-804.

3. Sartor O, de Bono J, Chi KN, et al. Lutetium-177-PSMA-617 for metastatic castration-resistant prostate cancer. *N Engl J Med.* 2021;385(12):1091-1103.

4. Hathi DK, Jones EF. (68)Ga FAPI PET/CT: Tracer uptake in 28 different kinds of cancer. *Radiol Imaging Cancer.* 2019;1:e194003.

5. Fendler WP, Stuparu AD, Evans-Axelsson S, et al. Establishing (177)Lu-PSMA-617 radioligand therapy in a syngeneic model of murine prostate cancer. *J Nucl Med.* 2017;58:1786-1792.

6. Loktev A, Lindner T, Burger EM, et al. Development of fibroblast activation protein-targeted radiotracers with improved tumor retention. *J Nucl Med.* 2019;60:1421-1429.

7. Jensen MM, Jorgensen JT, Binderup T, Kjaer A. Tumor volume in subcutaneous mouse xenografts measured by microCT is more accurate and reproducible than determined by 18F-FDG-microPET or external caliper. *BMC Med Imaging.* 2008;8:16.

8. Luckerath K, Stuparu AD, Wei L, et al. Detection threshold and reproducibility of (68)Ga-PSMA11 PET/CT in a mouse model of prostate cancer. *J Nucl Med.* 2018;59:1392-1397.

9. Sandstrom M, Garske-Roman U, Granberg D, et al. Individualized dosimetry of kidney and bone marrow in patients undergoing 177Lu-DOTA-octreotate treatment. *J Nucl Med.* 2013;54:33-41.

10. Delker A, Fendler WP, Kratochwil C, et al. Dosimetry for (177)Lu-DKFZ-PSMA-617: a new radiopharmaceutical for the treatment of metastatic prostate cancer. *Eur J Nucl Med Mol Imaging.* 2016;43:42-51.

11. Strigari L, Konijnenberg M, Chiesa C, et al. The evidence base for the use of internal dosimetry in the clinical practice of molecular radiotherapy. *Eur J Nucl Med Mol Imaging.* 2014;41:1976-1988.

12. Gafita A, Rauscher I, Retz M, et al. Early experience of rechallenge (177)Lu-PSMA radioligand therapy after an initial good response in patients with advanced prostate cancer. *J Nucl Med.* 2019;60:644-648.

13. Current K, Meyer C, Magyar CE, et al. Investigating PSMA-targeted radioligand Therapy efficacy as a function of cellular PSMA levels and intratumoral PSMA heterogeneity. *Clin Cancer Res.* 2020;26:2946-2955.

14. Sanchez-Felix M, Burke M, Chen HH, Patterson C, Mittal S. Predicting bioavailability of monoclonal antibodies after subcutaneous administration: Open innovation challenge. *Adv Drug Deliv Rev.* 2020;167:66-77.

15. Dou S, Smith M, Wang Y, Rusckowski M, Liu G. Intraperitoneal injection is not always a suitable alternative to intravenous injection for radiotherapy. *Cancer Biother Radiopharm.* 2013;28:335-342.

16. Bittner B, Richter W, Schmidt J. Subcutaneous administration of biotherapeutics: An overview of current challenges and opportunities. *BioDrugs.* 2018;32:425-440.

17. Viola M, Sequeira J, Seica R, et al. Subcutaneous delivery of monoclonal antibodies: How do we get there? *J Control Release.* 2018;286:301-314.

18. Wehrmann C, Senftleben S, Zachert C, Muller D, Baum RP. Results of individual patient dosimetry in peptide receptor radionuclide therapy with 177Lu DOTA-TATE and 177Lu DOTA-NOC. *Cancer Biother Radiopharm.* 2007;22:406-416.

19. Kabasakal L, AbuQbeitah M, Aygun A, et al. Pre-therapeutic dosimetry of normal organs and tissues of (177)Lu-PSMA-617 prostate-specific membrane antigen (PSMA) inhibitor in patients with castration-resistant prostate cancer. *Eur J Nucl Med Mol Imaging.* 2015;42:1976-1983.

20. Tylski P, Pina-Jomir G, Bournaud-Salinas C, Jalade P. Tissue dose estimation after extravasation of (177)Lu-DOTATATE. *EJNMMI Phys.* 2021;8:33.

Tables

Table 1. I.p. or s.c. application led to higher or equivalent tumor uptake compared to i.v injection. Mice with subcutaneous RM1-SSTR, RM1-PSMA or HT1080-FAP tumors were injected with ^{68}Ga-DOTATOC, ^{68}Ga-PSMA11 or ^{68}Ga-FAPI46. Absolute tumor uptake (%IA/g) at 1h and 4h p.i (*in vivo* PET), and 5h p.i. (*ex vivo* gamma counter) is given. Data are represented as mean %IA/g±SEM of *n*=6 mice/group. *p<0.05; **p<0.01.

RM1-SSTR (^{68}Ga-DOTATOC)							
	i.v.	**i.p.**	**s.c.**	**p-value i.v. vs. i.p.**	**p-value i.v. vs. s.c.**		
***in vivo* 1 h**	5.3 ± 0.6	9.9 ± 1.0	10.8 ± 1.6	p=0.0124*	p=0.0377*		
***in vivo* 4 h**	4.4 ± 0.7	8.6 ± 1.1	11.1 ± 2.0	p=0.0301*	p=0.0411*		
***ex vivo* 5 h**	2.9 ± 0.3	7.2 ± 1.1	6.5 ± 1.3	p=0.0197*	p=0.0827		
RM1-PSMA (^{68}Ga-PSMA11)							
	i.v.	**i.p.**	**s.c.**	**p-value i.v. vs. i.p.**	**p-value i.v. vs. s.c.**		
***in vivo* 1 h**	2.9 ± 0.2	3.0 ± 0.6	2.6 ± 0.4	p=0.9837	p=0.8297		
***in vivo* 4 h**	2.6 ± 0.2	2.6 ± 0.7	2.9 ± 0.5	p=0.9996	p=0.8289		
***ex vivo* 5 h**	3.3 ± 0.7	3.4 ± 0.8	3.9 ± 0.8	p=0.9954	p=0.8343		
HT1080-FAP (^{68}Ga-FAPI46)							
	i.v.	**i.p.**	**s.c.**	**p.o.**	**p-value i.v. vs. s.c**	**p-value i.v. vs. s.c**	**p-value i.v. vs. p.o.**
***in vivo* 1 h**	1.2 ± 0.2	2.0 ± 0.4	2.2 ± 1.1	0.1±0.03	p=0.3024	p=0.6732	p=0.0032**
***in vivo* 4 h**	1.0 ± 0.2	1.5 ± 0.3	1.1 ± 0.6	0.1±0.04	p=0.4559	p=0.9911	p=0.0087**
***ex vivo* 5 h**	1.0 ± 0.2	1.1 ± 0.1	1.4 ± 0.4	0.02±0.01	p=0.9805	p=0.7446	p=0.0058**

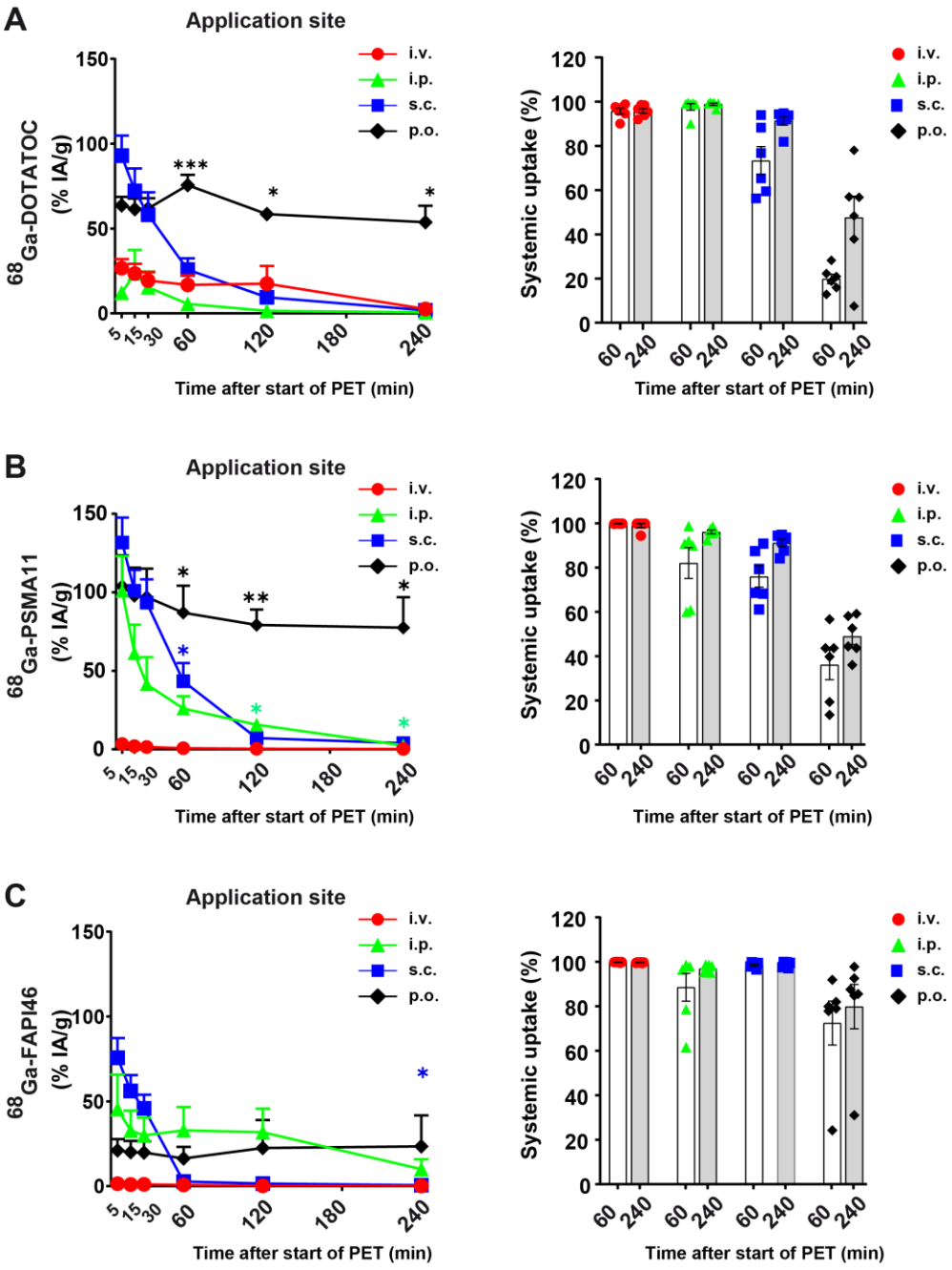

Figure 1. Activity at the application site and systemic availability over time in healthy mice. Retention of (A) ^{68}Ga-DOTATOC, (B) ^{68}Ga-PSMA11, and (C) ^{68}Ga-FAPI46 in healthy mice (n=6/group) at the application site. *Left panel*: Time activity curves illustrate radioligand dynamics at the application site for i.v., i.p., s.c., and p.o. application. *Right panel*: Relative systemic uptake of whole body VOI excluding application site VOI displayed in % of total body uptake. Each dot represents a mouse. Data are shown as mean+SEM. %IA/g: percent of the injected activity per gram. Asterisks indicate significance compared to i.v. application. *p<0.05; **p<0.01; ***p<0.001.

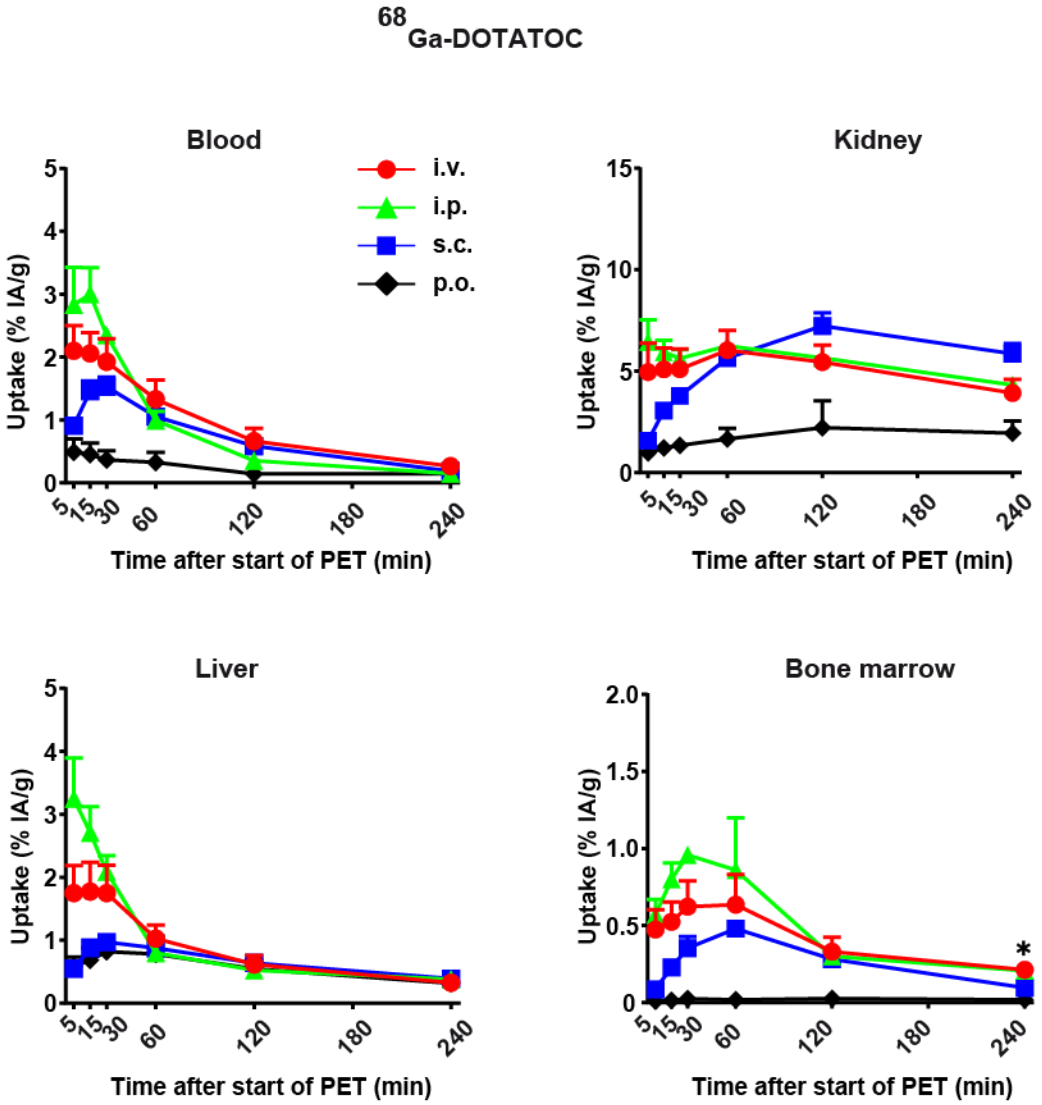

Figure 2. In healthy mice, organ biodistribution at ≥1h p.i following i.p. and s.c. radioligand application is nearly equivalent to i.v. injection. Healthy mice (*n*=6/group) underwent PET scans following i.v., i.p., s.c., and p.o. radioligand application, respectively, at minute 0-30 after start of PET and after 1h, 2h and 4h with subsequent sacrifice of animals. Time-activity curves illustrate *in vivo* PET biodistribution of ^{68}Ga-DOTATOC dynamics in VOIs at indicated times for i.v., i.p., s.c., and p.o. application. Data are shown as mean+SEM. %IA/g: percent injected activity per gram. Asterisks indicate significance compared to i.v. injection.*p<0.05.

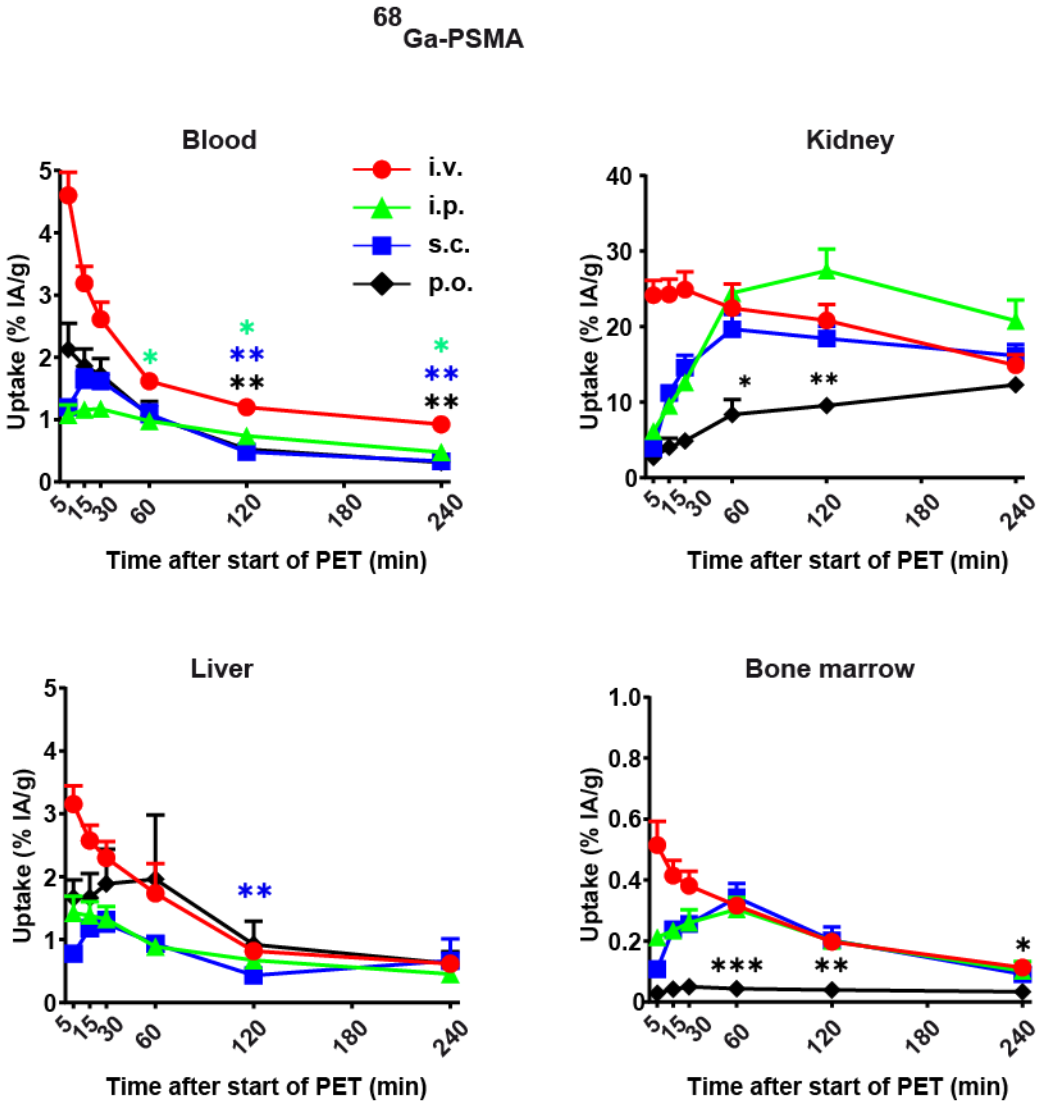

Figure 3. In healthy mice, organ biodistribution at ≥1h p.i following i.p. and s.c. radioligand application is nearly equivalent to i.v. injection. Healthy mice (*n*=6/group) underwent PET scans following i.v., i.p., s.c., and p.o. radioligand application, respectively, at minute 0-30 after start of PET and after 1h, 2h and 4h with subsequent sacrifice of animals. Time-activity curves illustrate *in vivo* PET biodistribution of ^{68}Ga-PSMA dynamics in VOIs at indicated times for i.v., i.p., s.c., and p.o. application. Data are shown as mean+SEM. %IA/g: percent injected activity per gram. Asterisks indicate significance compared to i.v. injection.*p<0.05; **p<0.01; ***p<0.001.

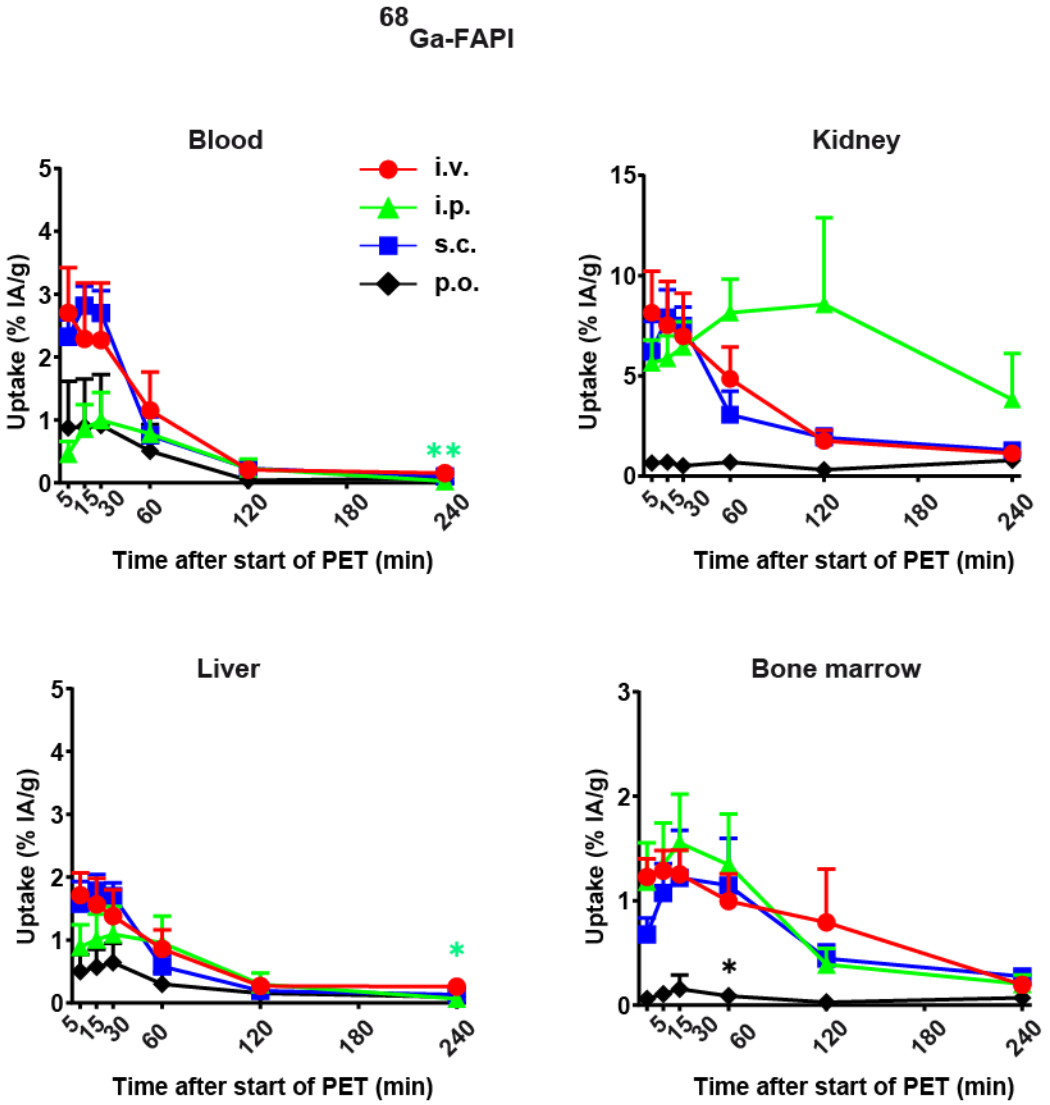

Figure 4. In healthy mice, organ biodistribution at ≥1h p. Healthy mice (*n*=6/group) underwent PET scans following i.v., i.p., s.c., and p.o. radioligand application, respectively, at minute 0-30 after start of PET and after 1h, 2h and 4h with subsequent sacrifice of animals. Time-activity curves illustrate *in vivo* PET biodistribution of ^{68}Ga-FAPI dynamics in VOIs at indicated times for i.v., i.p., s.c., and p.o. application. Data are shown as mean+SEM. %IA/g: percent injected activity per gram. Asterisks indicate significance compared to i.v. injection.*p<0.05; **p<0.01.

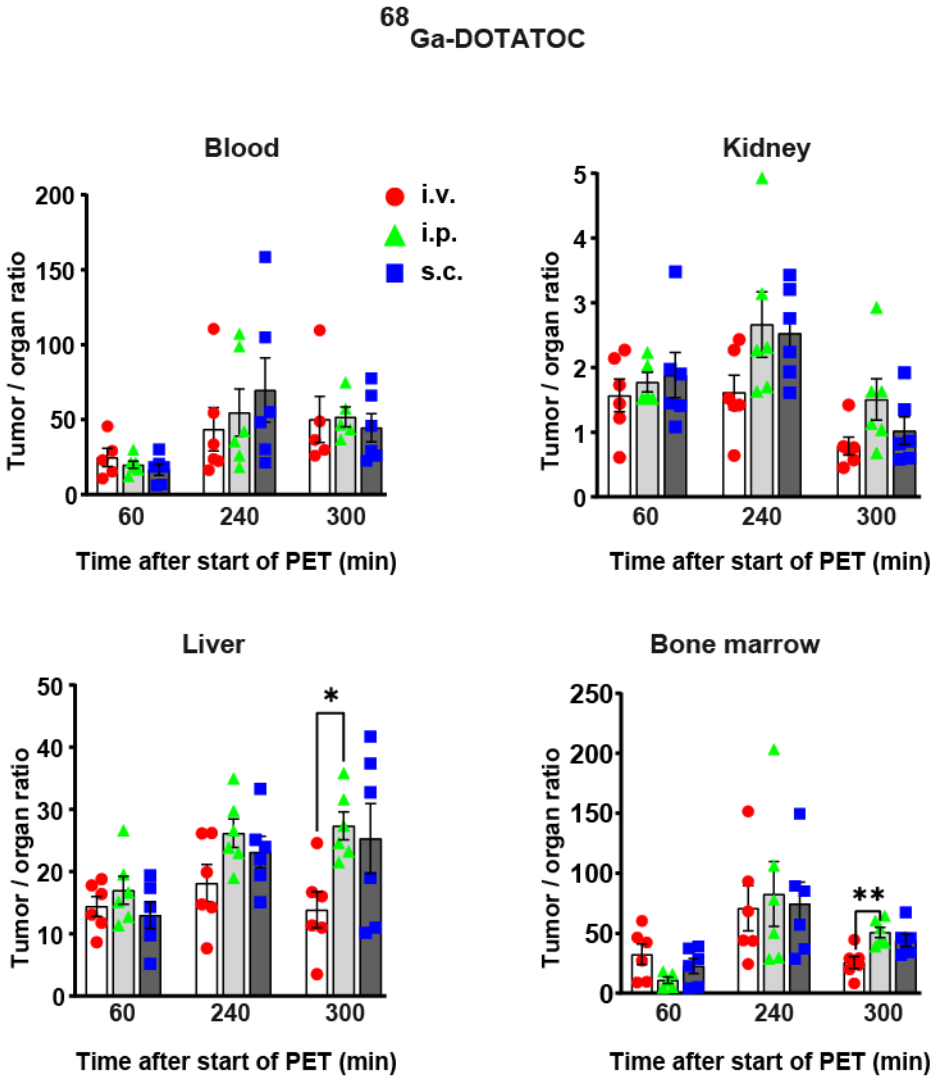

Figure 5. I.p. and s.c. radioligand application increase tumor-to-liver uptake compared to i.v. injection. Mice with subcutaneous RM1-SSTR tumors (*n*=6/group) with i.v., i.p. and s.c. application of ^{68}Ga-DOTATOC and PET scans after 1h and 4h, followed by sacrifice (5h) and subsequent assessment of radioactivity in organs and tumors by gamma counter. Plots show tumor-to-organ ratios after i.v., i.p. and s.c. of ^{68}Ga-DOTATOC. Each dot represents a mouse. Data are shown as mean±SEM. Asterisks indicate significance compared to i.v. injection. *p<0.05; **p<0.01.

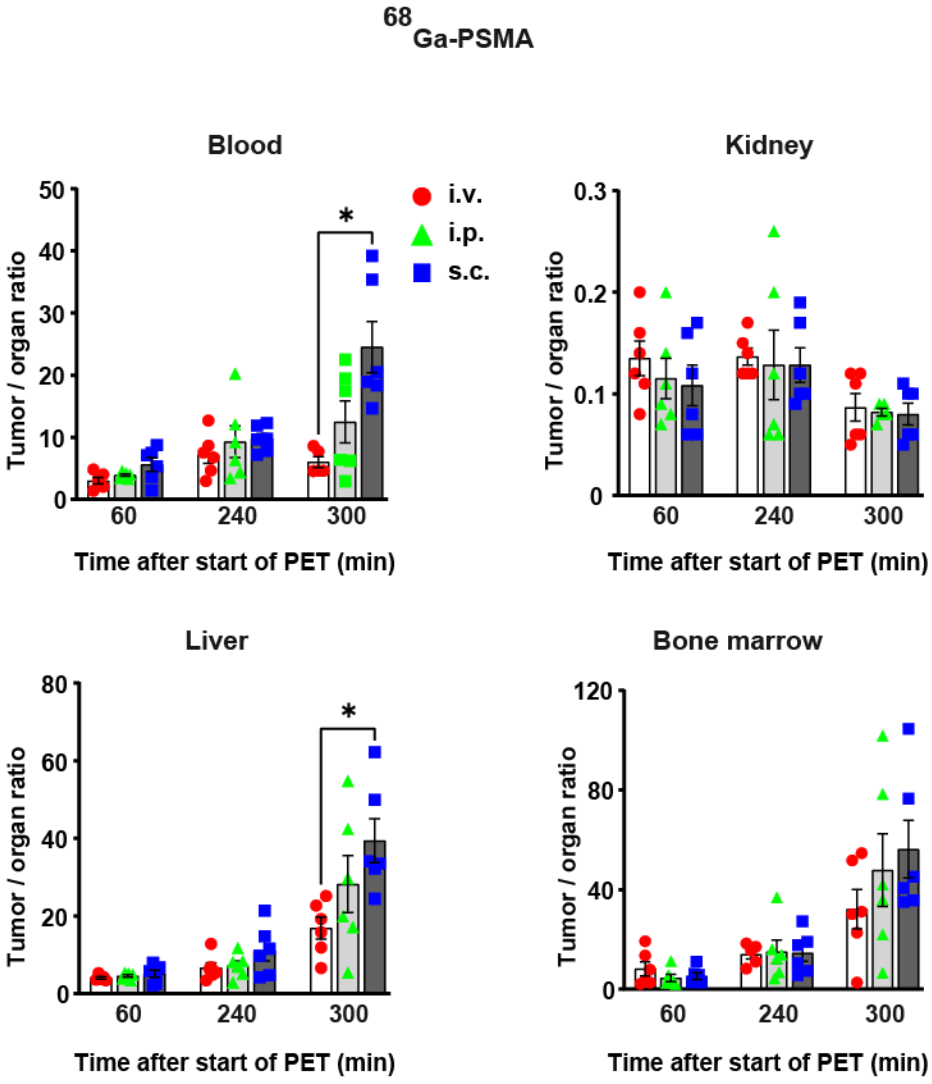

Figure 6. I.p. and s.c. radioligand application increase tumor-to-liver uptake compared to i.v. injection. Mice with subcutaneous RM1-PSMA tumors (*n*=6/group) with i.v., i.p. and s.c. application of ^{68}Ga-PSMA and PET scans after 1h and 4h, followed by sacrifice (5h) and subsequent assessment of radioactivity in organs and tumors by gamma counter. Plots show tumor-to-organ ratios after i.v., i.p. and s.c. of ^{68}Ga-DOTATOC. Each dot represents a mouse. Data are shown as mean±SEM. Asterisks indicate significance compared to i.v. injection. *p<0.05.

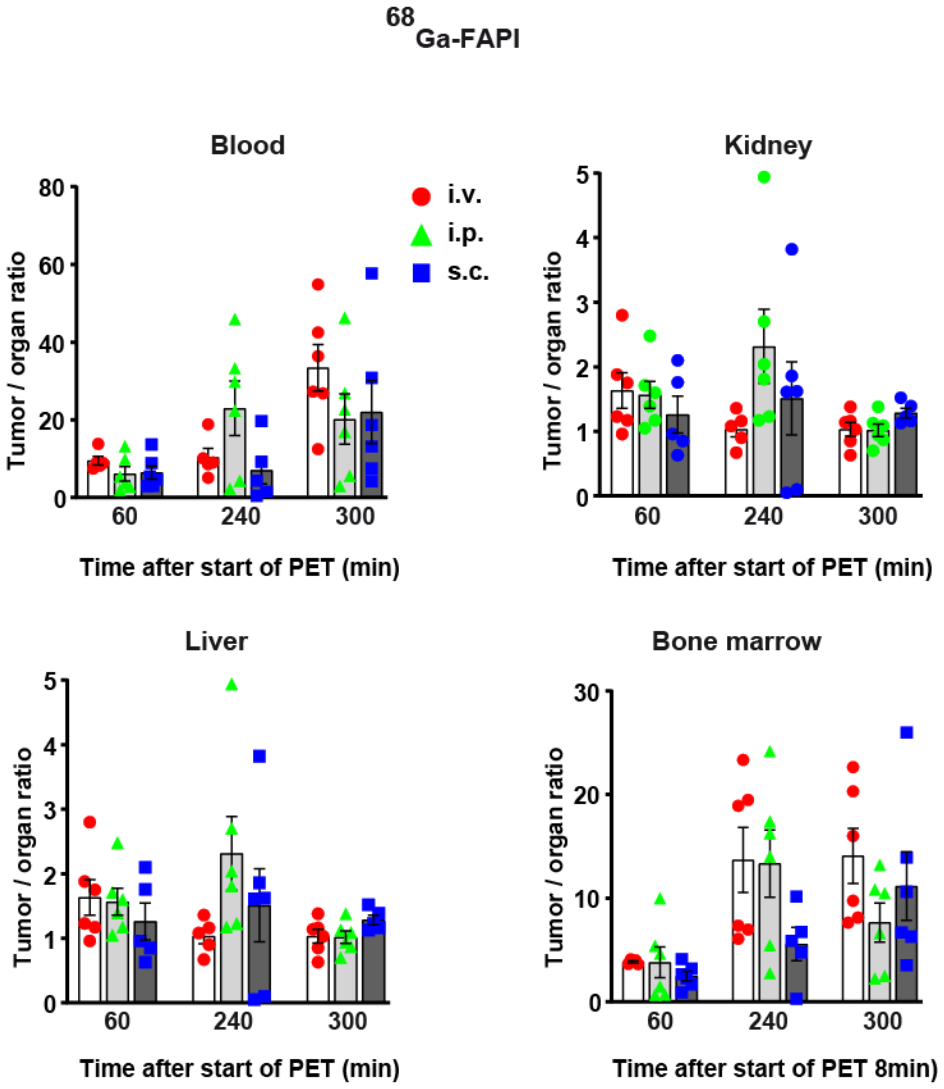

Figure 7. I.p. and s.c. radioligand application increase tumor-to-liver uptake compared to i.v. injection. Mice with subcutaneous HT-1080 tumors (*n*=6/group) with i.v., i.p. and s.c. application of ^{68}Ga-DOTATOC and PET scans after 1h and 4h, followed by sacrifice (5h) and subsequent assessment of radioactivity in organs and tumors by gamma counter. Plots show tumor-to-organ ratios after i.v., i.p. and s.c. of ^{68}Ga-DOTATOC. Each dot represents a mouse. Data are shown as mean±SEM.

GRAPHICAL ABSTRACT

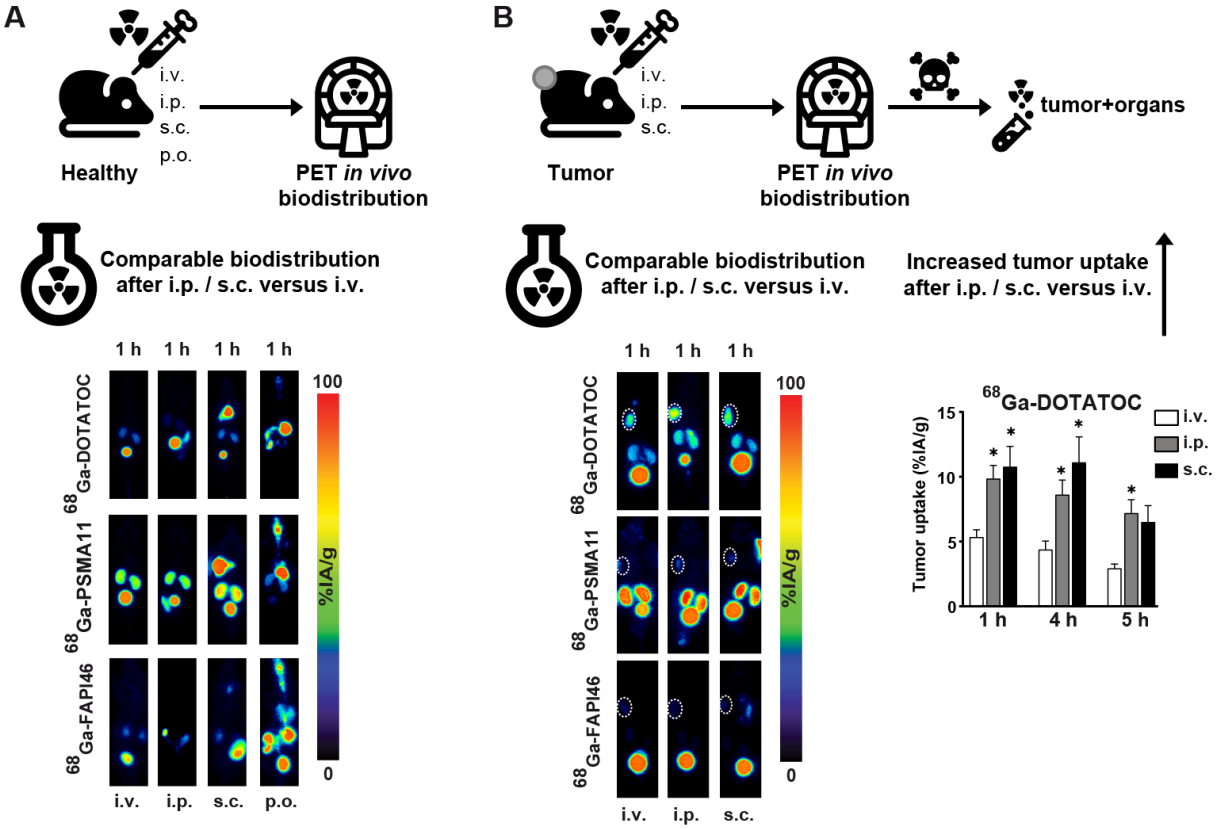

Supplement

Supplemental Tables

Supplemental Table 1. I.v., i.p., and s.c. injection led to near equivalent organ biodistribution of radioligands in healthy mice. Healthy mice were injected with ^{68}Ga-DOTATOC, ^{68}Ga-PSMA11, or ^{68}Ga-FAPI46, respectively. Absolute organ uptake is given as %IA/g at 1h and 4h p.i. (*in vivo* PET), and 5h p.i. (*ex vivo* gamma counter). Data represent mean %IA/g±SEM of *n*=6 mice/group. *p<0.05; **p<0.01.

	^{68}Ga-DOTATOC				
	i.v.	i.p.	s.c.	p-value i.v. vs. i.p.	p-value i.v. vs. s.c.
blood 1h	1.3 ± 0.3	1.0 ± 0.1	1.1 ± 0.1	0.7589	0.8431
blood 4h	0.3 ± 0.1	0.2 ± 0.02	0.2 ± 0.04	0.5639	0.8229
kidneys 1h	6.0 ± 1.0	6.2 ± 0.4	5.6 ± 0.5	0.9965	0.9837
kidneys 4h	3.9 ± 0.7	4.3 ± 0.2	5.9 ± 0.5	0.9393	0.1658
	^{68}Ga-PSMA11				
	i.v.	i.p.	s.c.	p-value i.v. vs. i.p.	p-value i.v. vs. s.c.
blood 1h	1.6 ± 0.1	1.0 ± 0.1	1.1 ± 0.1	p=0.0226*	p=0.0880*
blood 4h	0.9 ± 0.1	0.5 ± 0.1	0.3 ± 0.04	p=0.0394*	p=0.0065**
kidneys 1h	22.4 ± 3.2	24.4 ± 0.9	19.7 ± 2.0	p=0.9279	p=0.8773
kidneys 4h	14.9 ± 1.4	20.8 ± 2.8	16.1 ± 1.5	p=0.3040	p=0.9251
	^{68}Ga-FAPI46				
	i.v.	i.p.	s.c.	p-value i.v. vs. i.p.	p-value i.v. vs. s.c.
blood 1h	1.2 ± 0.6	0.8 ± 0.4	0.8 ± 0.3	p=0.9505	p=0.9345
blood 4h	0.2 ± 0.02	0.02 ± 0.01	0.1 ± 0.03	p=0.0036**	p=0.5326
kidneys 1h	4.9 ± 1.6	8.7 ± 1.7	3.1 ± 1.2	p=0.5065	p=0.8014
kidneys 4h	1.1 ± 0.2	3.8 ± 2.3	1.3 ± 0.2	p=0.6694	p=0.9513

Supplemental Figures

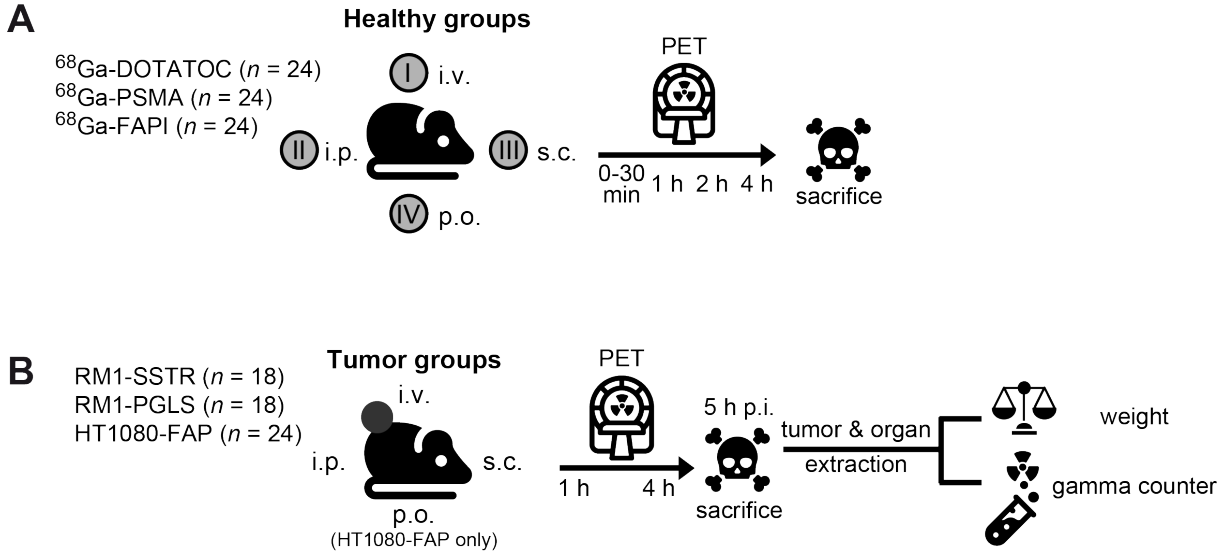

Supplemental Figure 1. Experimental design. (A) Healthy mice (*n*=6/group) underwent PET scans following i.v., i.p., s.c., and p.o. radioligand application, respectively, at minute 0-30 after start of PET and after 1h, 2h and 4h with subsequent sacrifice of animals. (B) Mice with subcutaneous RM1-SSTR, RM1-PSMA, or HT1080-FAP tumors (*n*=6/group) with i.v., i.p. and s.c. application of ^{68}Ga-DOTATOC, ^{68}Ga-PSMA11, or (C) ^{68}Ga-FAPI46, respectively underwent PET scans after 1h and 4h, followed by sacrifice (5h) and subsequent assessment of radioactivity in organs and tumors by gamma counter.

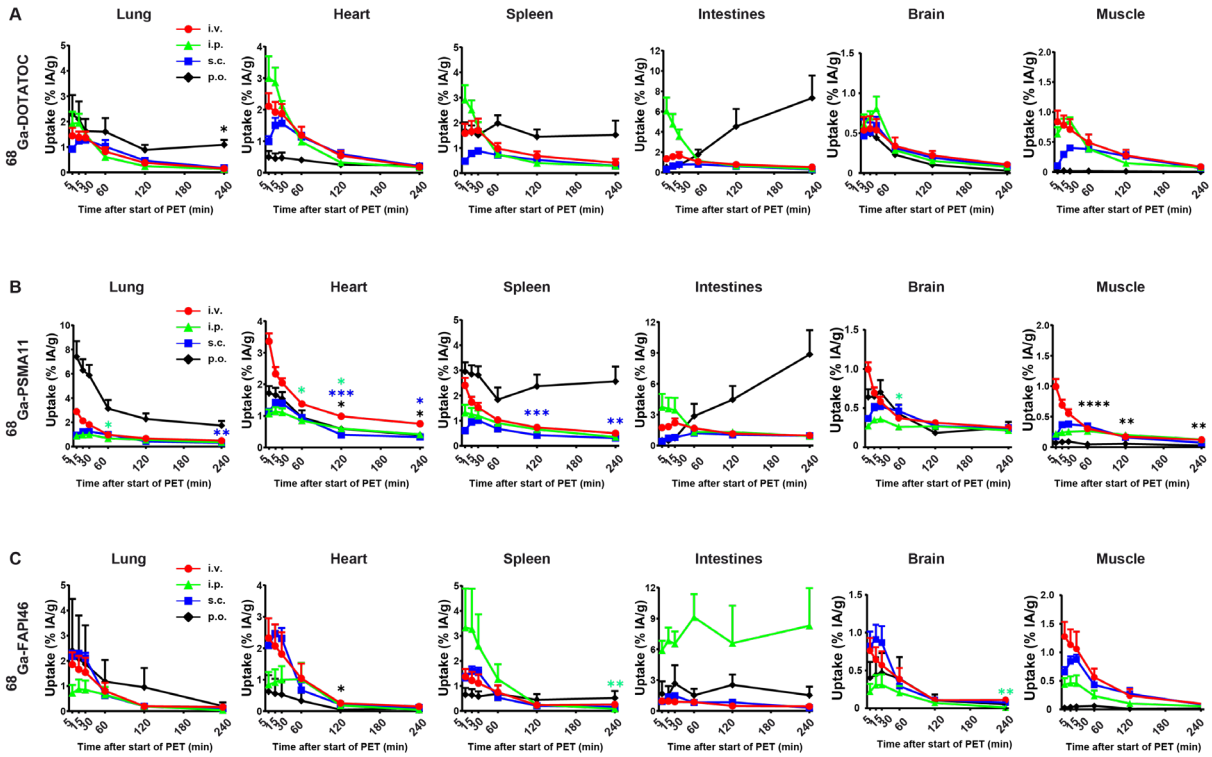

Supplemental Figure 2. Near equivalent radioligand organ biodistribution for i.p. and s.c. compared to i.v. injection in healthy mice. *In vivo* PET biodistribution of ^{68}Ga-ligands in healthy mice (*n*=6/group). PET scans with (A) ^{68}Ga-DOTATOC, (B) ^{68}Ga-PSMA11, and (C) ^{68}Ga-FAPI46. Time-activity curves illustrate radioligand dynamics in selected organ VOIs at indicated time points for i.v., i.p., s.c., and p.o. application. Data are shown as mean+SEM. %IA/g: percent of the injected activity per gram. Asterisks indicate significance compared to i.v. application route. *p<0.05; **p<0.01; ***p< 0.001; ****p<0.0001.

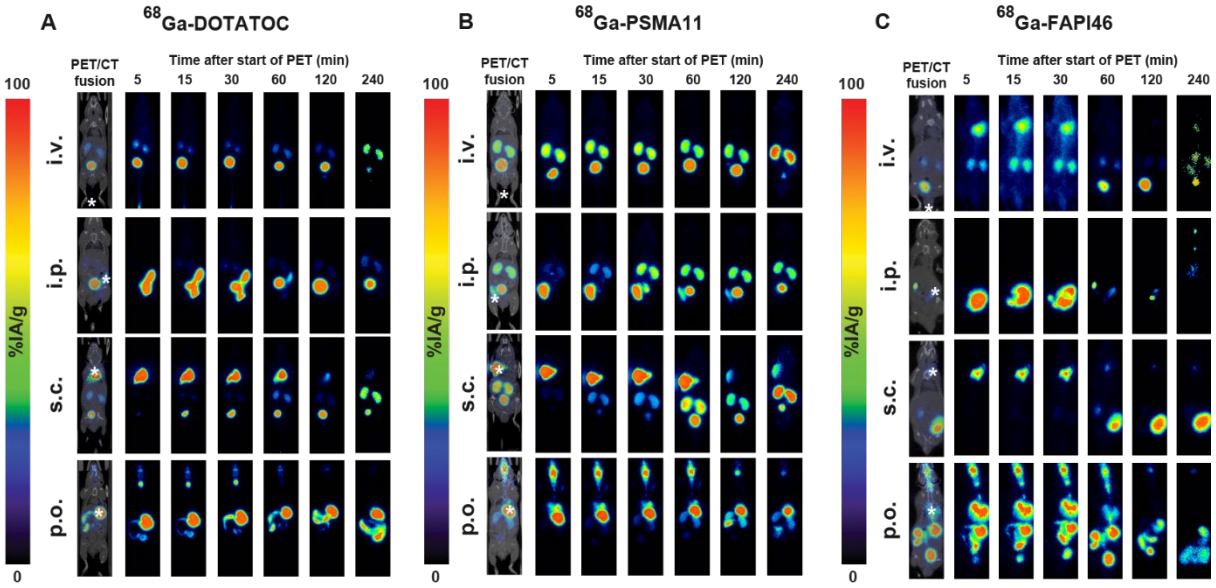

Supplemental Figure 3. PET biodistribution of ^{68}Ga-ligands in healthy mice. Whole body maximum intensity projections of one representative mouse out of *n*=6/group for each application route after injection of ^{68}Ga-labelled ligands. (A) ^{68}Ga-DOTATOC, (B) ^{68}Ga-PSMA11, and (C) ^{68}Ga-FAPI46 after i.v., i.p., s.c., and p.o. application in healthy mice. Asterisks indicate the injection site.

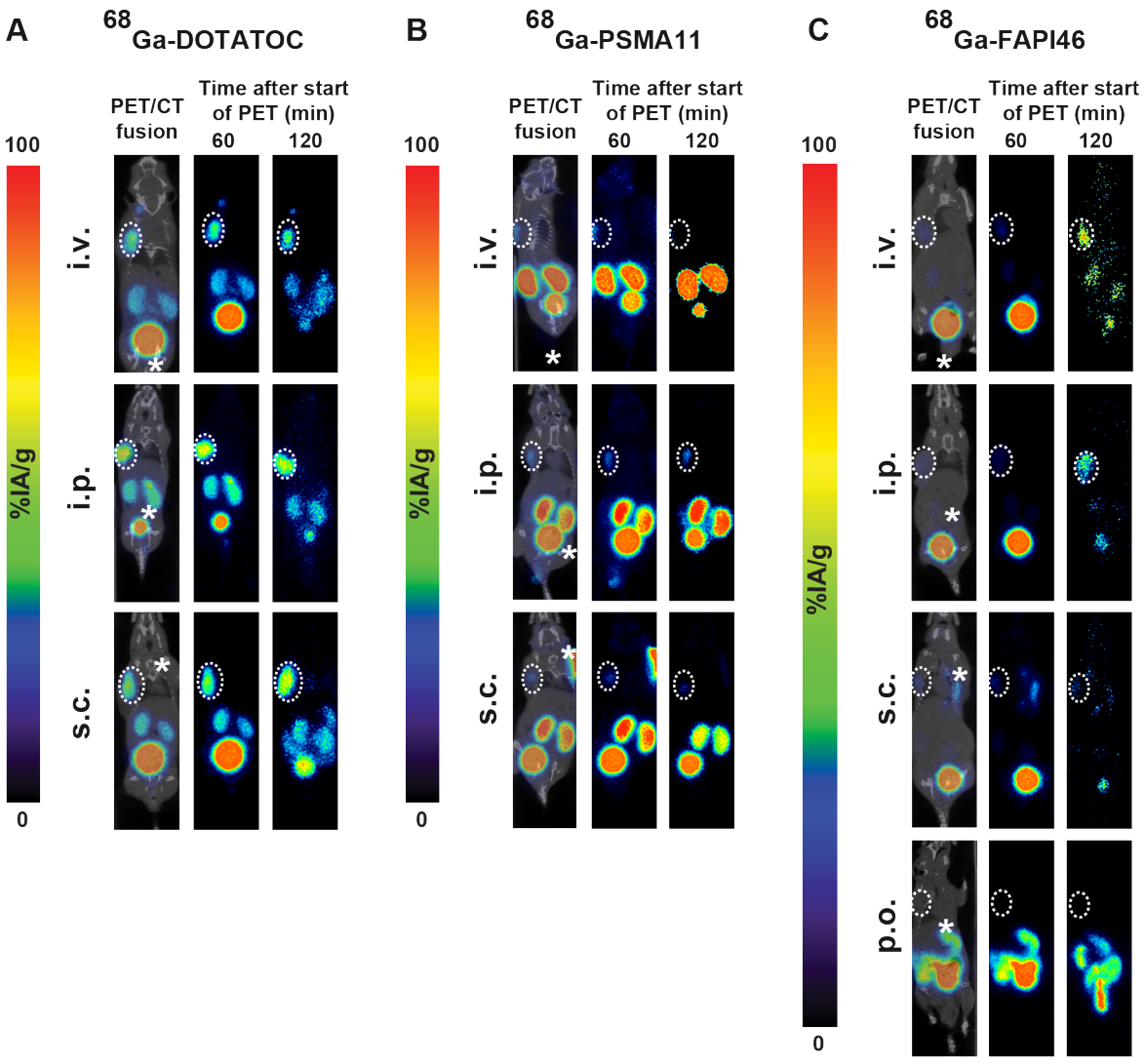

Supplemental Figure 4. PET biodistribution of ^{68}Ga-ligands in tumor-bearing mice. Whole body maximum intensity projections of one representative mouse out of *n*=6/group for each application route 1h and 4h after injection of ^{68}Ga-labelled ligands. (A) ^{68}Ga-DOTATOC, (B) ^{68}Ga-PSMA11, and (C) ^{68}Ga-FAPI46 via i.v., i.p., and s.c. application in RM1-SSTR-, RM1-PSMA-, or HT1080-FAP-tumor-bearing mice with additional p.o. application, respectively. Asterisks indicate the injection site; dashed circles indicate subcutaneous tumor in the right shoulder region.

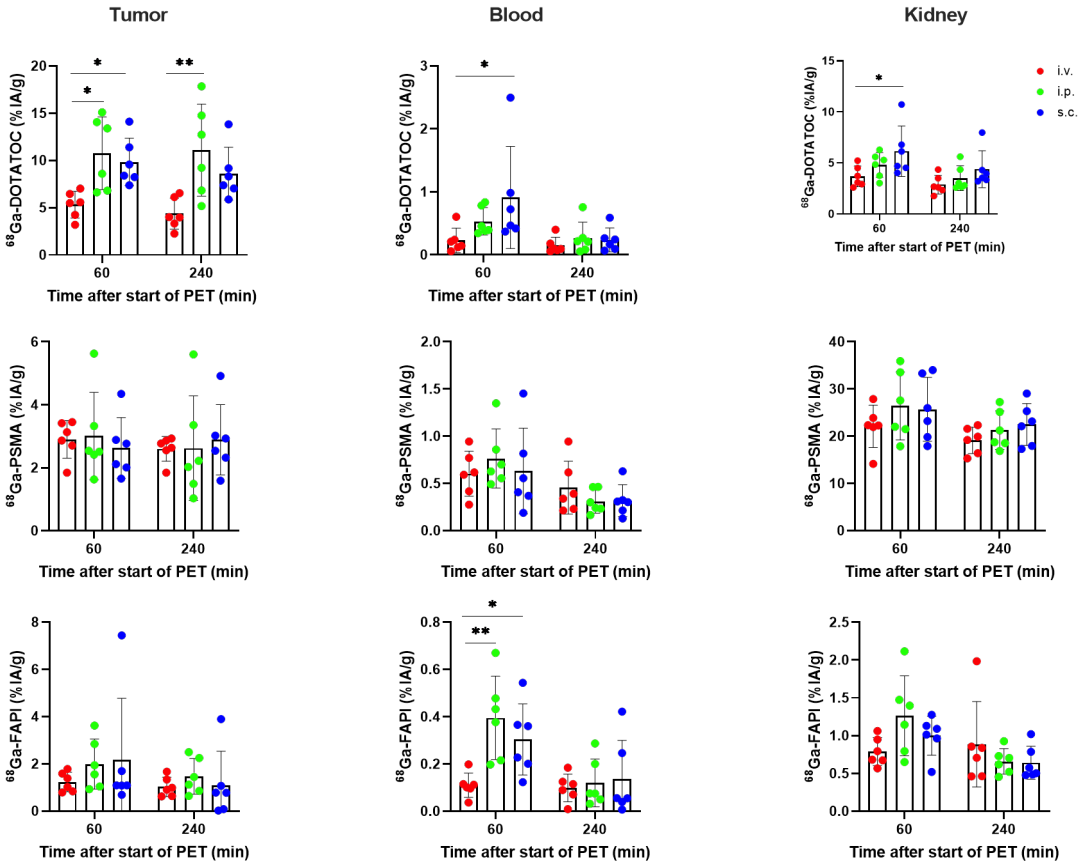

Supplemental Figure 5. PET biodistribution of ^{68}Ga-ligands in tumor-bearing mice. *In vivo* PET uptake of ^{68}Ga-ligands in tumor-bearing mice (*n*=6/group). after ^{68}Ga-DOTATOC, ^{68}Ga-PSMA11, and ^{68}Ga-FAPI46. Bars illustrate radioligand uptake in selected organ VOIs at indicated time points for i.v., i.p., and s.c. application. Data are shown as mean±SD. %IA/g: percent of the injected activity per gram. Asterisks indicate significance compared to i.v. application route. *p<0.05; **p<0.01.

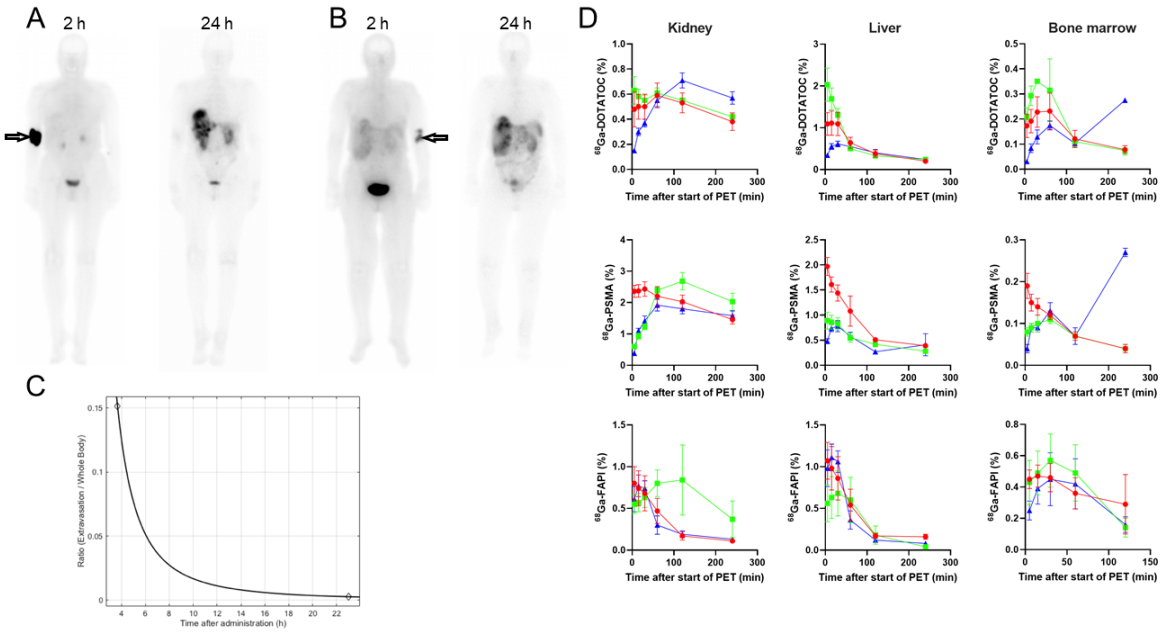

Supplemental Figure 6. Anterior whole-body planar images of ^{177}Lu-DOTATOC distribution 2h and 24h after paravenous infusion (arrow) of the radioligand in two patients (A and B). Radioligand absorption in patient A occurs with a half-life of 3.3 hours (C). Extrapolation from mice to humans suggests comparable biodistribution of ^{68}Ga-radioligands in healthy organs (D). Data are shown as mean±SEM.